

# Performance of silica fume-calcium hydroxide mixture as a repair material

V. Kasselouri, N. Kouloumbi \*, Th. Thomopoulos

*Chemical Engineering Department, National Technical University of Athens, 9 Heron Polytechniou Str, Athens 15 780, Greece*

Received 10 February 2000; accepted 9 November 2000

---

## Abstract

The aim of this experimental work was to investigate the performance of a special concrete repair material. The use of silica fume (SF)-Ca(OH)<sub>2</sub> mixture, with and without cement addition in reinforced mortars has been studied. The examination of the hydration reaction progress by X-Ray Diffraction (XRD), Differential Thermal Analysis-Thermogravimetry (DTA-TG), and Scanning Electron Microscopy (SEM) analysis of SF-Ca(OH)<sub>2</sub> mixture with various cement ratios, shows that calcium silicate hydrate is formed in a desired extent. Damaged specimens repaired by the above-mentioned materials also showed low carbonation depth and the lowest corrosion rate, close to of undamaged specimens. This is attributed to the formation of C-S-H compounds at the interface between these mixtures and cement mortar, resulting in the creation of good binding properties of the repair materials. © 2001 Elsevier Science Ltd. All rights reserved.

**Keywords:** Concrete; Reinforcement corrosion; Repair; Silica fume; Portlandite

---

## 1. Introduction

Hydrated cement is a porous solid, which usually provides good protection against corrosion of reinforced steel bars but, nevertheless, corrosion remains the most common cause of deterioration. In the alkaline pore solution in set cement (pH 12.5–13.5), a protective oxide film is formed over the steel, rendering it passive [1–3].

Failure of the reinforced concrete structures occurs when the protective oxide film is destroyed by carbonation or by penetration of aggressive ions such as chloride ion to the steel surface [2,4,5]. In sea water the penetration of chloride ions is faster than that of CO<sub>2</sub> and makes the CO<sub>2</sub> influence weaker [6]. The presence of chloride ions raises the pH required to stabilize the passive film to a value which may exceed that of a saturated calcium hydroxide solution so stimulating corrosion [1]. Between the two principal factors that characterize the deterioration process of concrete structures due to chloride corrosion, the diffusion of chloride ions dominates the generation of corrosion, while the diffusion of oxygen dominates its rate [7].

Carbonation, being a rather slow process, induces rebars, corrosion only in constructions with very thin concrete cover, high porosity, shrinkage cracks and so forth [8]. The steel rebars corrosion onset, the time interval before the attack starts and the rate by which it proceeds are dependent on factors influenced by the chemistry of cement, mineral additions, water to binder ratio, curing and environmental conditions [4,6,9–11].

Although concrete possesses unique durability properties, after an incubation period corrosion is triggered, imposing an increasing need for maintenance and repair.

As it is well known, there are a wide range of cementitious repair mortars based on cement and components similar to those of concrete. The composition of repair mortars could sometime consist of more than one type of cement (i.e. special cement, like ultra-fine alumina cement) together with additions (i.e. silica fume, slag or fly ash), aggregates (normal, lightweight and special types, fillers), admixtures, such as plasticizers, air entrainers and accelerators, polymer additives and fine polymer fibers [12–14]. It is normally impossible to get information on the exact composition of a repair mortar or on many of the components used in it.

In the present work, the efficiency of the use of silica fume (SF)-Ca(OH)<sub>2</sub> mixture with and without cement addition, as materials to repair reinforced concrete

\* Corresponding author. Fax: +30-018-35-906.

E-mail address: koni@orfeas.chemeng.ntua.gr (N. Kouloumbi).

structures, instead of conventional cement-SF mixtures is examined. These materials have been tested because the small particles of amorphous  $\text{SiO}_2$  in the SF powder react directly with  $\text{Ca}(\text{OH})_2$ , resulting in pure calcium silicate hydrates, in antithesis with cement-SF reaction which leads to a variety of hydrates (calcium silicate hydrates, aluminum silicate hydrates, ettringite, etc.) having different hydraulic factors [15]. Furthermore the rate of SF-Ca(OH)<sub>2</sub> reaction leads to better crystallization of the calcium silicate hydrates leading them to more stable structures. Further, the use of industrial by-products, such as SF, offers a low-priced solution to the environmental problem of depositing industrial waste [16].

It is aimed covering at the imperfections or defects (pores, cracks, etc.) of the structure, by these mixtures, from the early stage of its life so that the basic requirement for structural integrity of the structure can be fulfilled. This can result in an extended initiation period of the corrosion process depending also on factors, such as hydration products of the mixtures and their affinity with those of the cement, the interrelation between mixture and the surface of the imperfections under repair or more generally, on the characteristics of the creating interface.

## 2. Materials and techniques

The cement used in this work was an Ordinary Portland Cement (I45, BS 2:1996). The steel bars used were St200 type. Their chemical composition is shown in Table 1. Calcareous sand with a typical gradation of 0–0.2 mm (10% by wt) 0.2–1 mm (30% by wt) and 1–5 mm (60% by wt) and drinking water were also used. The composition of mortar specimens is given in Table 2.

Table 1  
Chemical composition of cement, silica fume and steel bars

Cement (Wt%)	Silica fume		Steel bar		
	(Wt%)	(Wt%)	(Wt%)		
$\text{SiO}_2$	20.64	$\text{SiO}_2$	90.90	Fe	99.23
$\text{Al}_2\text{O}_3$	4.67	$\text{Al}_2\text{O}_3$	1.12	Mn	0.56
$\text{Fe}_2\text{O}_3$	3.85	$\text{Fe}_2\text{O}_3$	1.46	S	0.07
CaO	64.55	CaO(total)	0.69	C	0.11
Mgo	2.00	CaO(free)	0.024	P	0.03
K <sub>2</sub> O	0.57	Mgo	0.77		
Na <sub>2</sub> O	0.10	SO <sub>3</sub>	0.38		
SO <sub>3</sub>	2.50	LOI	3.00		
SUM	98.87				
LSF	98.07				
SIM	2.42				
ALM	1.21				

Table 2  
Composition of mortar specimens

Composition ratio by wt				
OPC	Sand 0–0.2 mm	Sand 0.2–1 mm	Sand 1–5 mm	Water
1	0.38	1.14	2.27	0.72

The repair mixtures consisted of densified silica fume of Norwegian origin (SF), (amorphous  $\text{SiO}_2$  > 90% wt – Table 1) and commercial calcium hydroxide. The calcium hydroxide was in slurry form containing 50% water.

The dimensions and the position of the steel bar in test specimens considered for the present study are shown in Fig. 1. The steel bars were machined on a lathe to a final diameter of 10 mm. They were washed with water, then immersed for 15 min in a strong solution of HCl with an organic corrosion inhibitor, washed thoroughly with distilled water to eliminate traces of the corrosion inhibitor and/or chloride ions. Following that, they were cleaned with acetone and then weighted to 0.1 mg.

The moulds with the specimens after casting were stored at an ambient temperature for 24 h. After the specimens were demolded the top surface of the specimen was insulated with an epoxy resin. The steel surface in contact with mortar was equal to 2276.5 mm<sup>2</sup>. Thereafter they were stored in the curing room ( $RH = 98 \pm 2\%$ ,  $T = 19 \pm 1^\circ\text{C}$ ) for 28 days.

At the end of the curing, a hole of 5 mm in diameter, was drilled in each lateral side of the specimen at a height corresponding to the middle of the embedded steel bar and to a depth up to 7 mm from the surface of the bar (Fig. 1). Holes were filled by one of the mixtures given in Table 3. All mixtures were in paste form. Consequently the damage of the specimens should have such dimensions to allow a complete intrusion of the repair material. The minimum satisfying diameter found in this case was 4–5 mm. In order to improve the setting

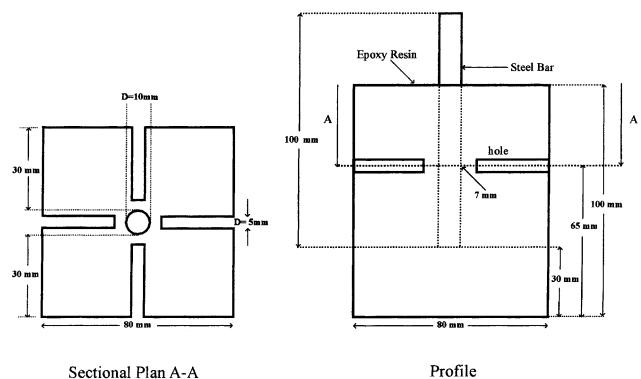


Fig. 1. Schematic representation of reinforced mortar specimens.

Table 3  
Composition of repair mixtures

Component	Code name of repaired specimens		
	Composition wt%		
	C	D	E
Silica fume	21.3	20.7	20.0
$\text{Ca(OH)}_2$	78.7	76.3	74.0
OPC	0.0	3.0	6.0

time of the SF- $\text{Ca(OH)}_2$  mixture, small amounts of cement have been added. It is known [17] that when  $\text{SiO}_2$  and  $\text{Ca(OH)}_2$  react to form C-S-H compounds the rate of this reaction is lower than that of the hydration of the calcium silicate compounds contained in the cement, resulting in different setting times.

Reference undamaged specimens (code name A) and specimens with unfilled holes (code name B) were also used. Finally, an adequate number of all types of specimens were immersed in 3.5% NaCl solution for corrosion potential, weight loss and potentiodynamic polarization measurements while those for carbonation depth measurements were stored at ambient condition.

The study of the hydration products of the repair mixtures at predetermined ages by X-Ray Diffraction (XRD) and Differential Thermal Analysis-Thermogravimetry (DTA-TG) was performed by a D5000 SIEMENS Diffractometer as well as by DTA-TG instrument, type STA 409 NETZSH. The samples were prepared after interruption of the hydration by a treatment with acetone and diethylether followed by grinding to a fine powder (sieve < 54  $\mu\text{m}$ ). For the study by Scanning Electron Microscopy (SEM), a JEOL 6100 Electron Microscope has been used. All the above analyses were performed on specimens immersed in tap water in order to avoid probable interference of hydration products with chloride ions at the corrosion environment used.

The durability of the specimens was evaluated by measuring the corrosion potentials on the steel, the carbonation depth and the corrosion rate of the rebars by anodic potentiodynamic polarization measurements and by weight loss measurements.

The corrosion potentials of the rebars were measured versus immersion time using a saturated calomel electrode (SCE) as reference electrode. The carbonation depth of the specimens was determined by the phenolphthalein method as recommended by RILEM (RILEM CPC-18) on broken mortar pieces at the interface mortar-repair mixture. In damaged but not repaired specimens carbonation depth was measured on broken mortar pieces at one lateral axis of the hole.

The potentiodynamic polarization measurements were performed in a CMS 100 system (Corrosion Measurement System) by Garmy Instrument, using 3.5% NaCl solution mechanically stirred as corrosion medium. The auxiliary electrode consisted of two cylindrical graphite rods. Before each measurement the potential was recorded until it reached an almost stable value that was the corrosion potential  $E_{\text{corr}}$ . Then the working electrode was polarized in a range of about -250 to +250 mV of  $E_{\text{corr}}$ . The resulting current was plotted on a logarithmic scale against the applied potential on a normal scale. Since the relatively large potential scale of this method may change the surface of the steel bars and may induce artificial corrosion, each experiment was performed using another specimen.

### 3. Results and discussion

The hydration products of SF- $\text{Ca(OH)}_2$ , as well as SF- $\text{Ca(OH)}_2$ -cement mixtures at the age of 7 days, 28 days, 6 months and 1 year have been examined by XRD. Fig. 2 presents the XRD patterns of hydrated repair mixtures after 28 days, 6 months and one year of hydration. At all ages of hydration the main compounds

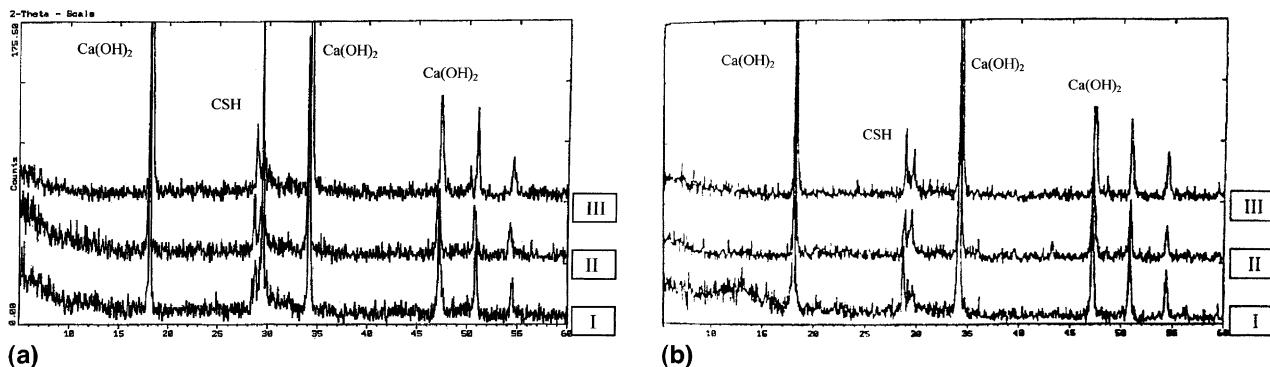


Fig. 2. (a) XRD patterns of hydrated repair mixtures after a 28-day hydration I. Pure SF- $\text{Ca(OH)}_2$  mixture II. SF- $\text{Ca(OH)}_2$  – 3% wt OPC mixture III. SF- $\text{Ca(OH)}_2$  – 6% wt OPC mixture; (b) XRD patterns of hydrated repair mixtures after 6 months and 1 year I. Pure SF- $\text{Ca(OH)}_2$  mixture after a 6-month hydration II. SF- $\text{Ca(OH)}_2$  – 3% wt OPC mixture after a 6 months hydration. III. SF- $\text{Ca(OH)}_2$  – 3% wt OPC mixture after 1 year hydration.

observed are  $\text{Ca}(\text{OH})_2$  in the form of portlandite (18.1, 34.2, 47.5° 2θ), small amount of  $\text{CaCO}_3$  (29.4° 2θ) due to carbonation of  $\text{Ca}(\text{OH})_2$  and calcium silicate hydrates in the form of tobermorite (11° 2θ). From the first ages the formation of calcium silicate hydrates in the form of tobermorite 11 and 14 Å as well as in the form of  $2\text{CaSiO}_3 \cdot 3\text{H}_2\text{O}$  (Riverveldite 5.5, 7.0, 10.0, 28.7, 29.8, 31.0° 2θ) can be observed, either in the mixtures of SF- $\text{Ca}(\text{OH})_2$ , or in the SF- $\text{Ca}(\text{OH})_2$ -cement ones [18].

At the ages of 28 days, 6 months and 1 year the amount of calcium silicate hydrates is equal to or slightly more in the mixture of SF- $\text{Ca}(\text{OH})_2$ , in comparison with that in the mixtures containing cement. This observation suggests that the addition of a small amount of cement (i.e. up to 6% wt) helps only in the improvement of the setting time of the mixtures. The existence of a remarkable amount of unreacted  $\text{Ca}(\text{OH})_2$ , even after a year of hydration, indicates the slow rate of the reaction between  $\text{Ca}(\text{OH})_2$  and the  $\text{SiO}_2$  contained in the silica fume.

The investigation of binding between the main mass of damaged specimen and the repair material was carried out by Scanning Electron Microscopy. Fig. 3 presents a mortar part adjacent to the repaired hole after 2 and 18 months of hydration. A cluster of thin crystals of calcium silicate hydrate is observed.

The microanalysis of the crystals of Fig. 3(a) showed that they contain 32.33% CaO and 31.55%  $\text{SiO}_2(\text{CaO}/\text{SiO}_2) \cong 1$ . The crystals have slightly rounded edges, which indicates rapid crystallization. After 18 months of hydration (Fig. 3(b)), a better crystallization of the C-S-H crystals as well as production of hydrated compound into the pores of the total mass are observed. In Figs. 4 and 5 the SEM of hydrated repair material (SF- $\text{Ca}(\text{OH})_2$ ) is presented.

Fig. 4(a) shows a grain of partly hydrated silica fume that has been formed in the boundaries of the grain calcium silicate hydrate. A focus on this boundaries'

area is presented in Fig. 4(b). The microanalysis of Fig. 4(a) gave as a result 52.39% CaO and 46.54%  $\text{SiO}_2(\text{CaO}/\text{SiO}_2) \cong 1.26$ . In the center of the grain's surface a cover of  $\text{Ca}(\text{OH})_2$  is observed (75.92% CaO and 22.04%  $\text{SiO}_2$ ;  $\text{CaO}/\text{SiO}_2 \cong 3.78$ ). The crystals shown in Fig. 4(b) have a needle-like form which indicates a better crystallization of the calcium silicate hydrates than that of cement mortar. Fig. 5(a) shows the SEM of an 18-month hydrated SF- $\text{Ca}(\text{OH})_2$  mixture. In Fig. 5(a) a 200 μm SF grain seems to remain partially reacted. In the main surface of the grain cracks are observed while in the boundaries (Fig. 5(b)) an appropriate amount of C-S-H ( $\text{CaO}/\text{SiO}_2 \cong 1.12$ ) has been formed.

As it concerns the interface between the damage mortar and the repair material, sufficient formation of C-S-H can be observed (Figs. 6(a) and (b)). The form of the crystals is more similar to that of the hydrated cement mortar. After 18 months of hydration the structure of the SF- $\text{Ca}(\text{OH})_2$  mixture (Fig. 6(b) upper left part) is very condensed and well adhered on the mortar mass (Fig. 6(b) down right part).

DTA-TG measurement has been performed on a 3-month hydrated SF- $\text{Ca}(\text{OH})_2$  mixture. The thermogram (Fig. 7) shows three endothermic peaks at 125–130°C, 520°C and 780°C, corresponding to the dehydration of calcium silicate hydrates, the dehydration of  $\text{Ca}(\text{OH})_2$  and the decarbonation of  $\text{CaCO}_3$  formed during the preparation of the sample. Respectively, the exothermic peak at 975°C shows a crystallographic transformation of the anhydrous tobermorites [18,19].

The corrosion activity of the reinforcing steel can be qualitatively estimated, regardless of the specimen size or the depth of the concrete cover, by monitoring the change in the corrosion potential of the steel bars with the time of exposure. In Fig. 8, the  $E_{\text{corr}}$  trend in the different types of samples is shown. All specimens, immediately after immersion in chloride environment

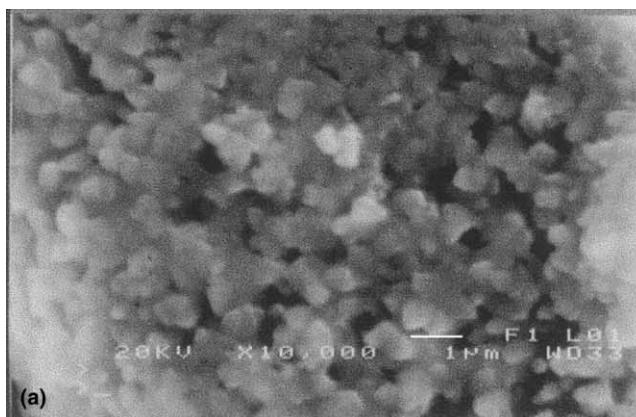
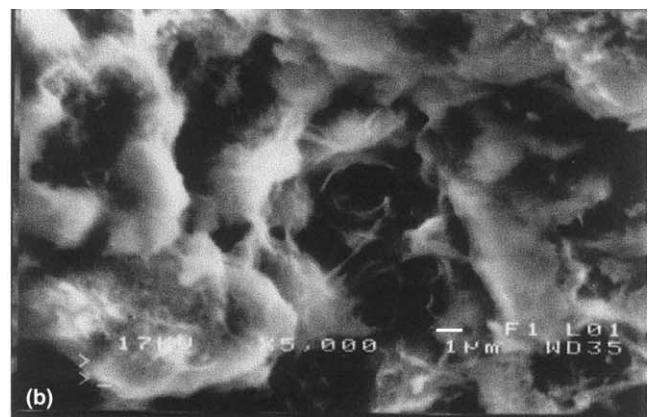


Fig. 3. (a) SEM of a 2 months hydrated cement mortar ( $M \times 10,000$ ) (b) SEM of an 18 month hydrated cement mortar ( $M \times 5000$ ).



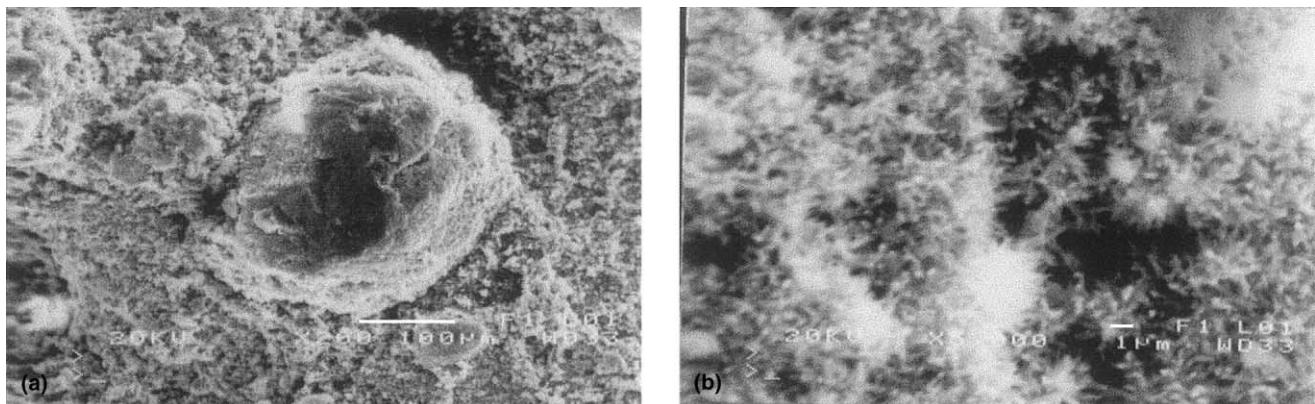


Fig. 4. (a) SEM of 28 days hydrated repair material SF-Ca(OH)<sub>2</sub> (M × 200) (b) SEM of 28 days hydrated repair material SF-Ca(OH)<sub>2</sub>. Details of the grain's boundaries (M × 5000).

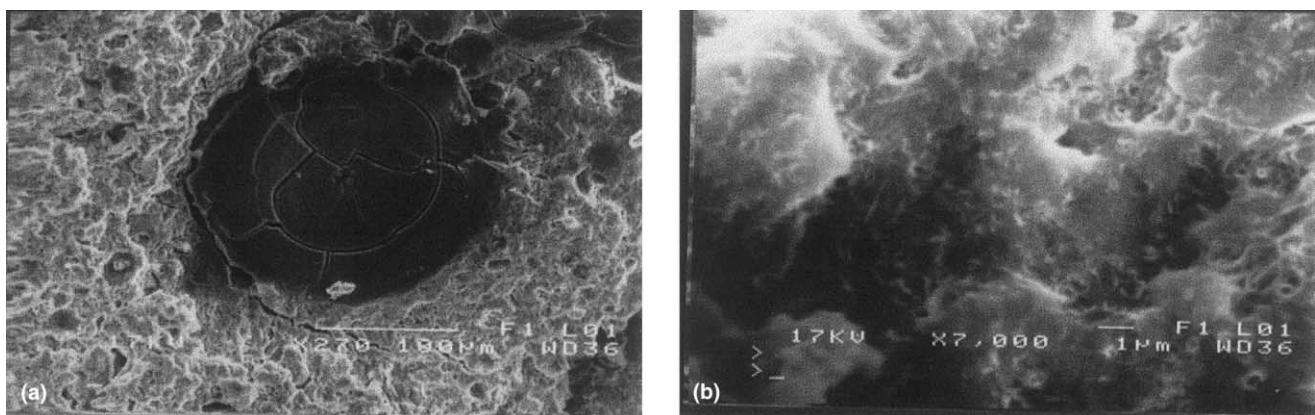


Fig. 5. (a) SEM of 18 months hydrated repair material SF-Ca(OH)<sub>2</sub> (M × 270) (b) SEM of 18 months hydrated repair material SF-Ca(OH)<sub>2</sub> (M × 7000).

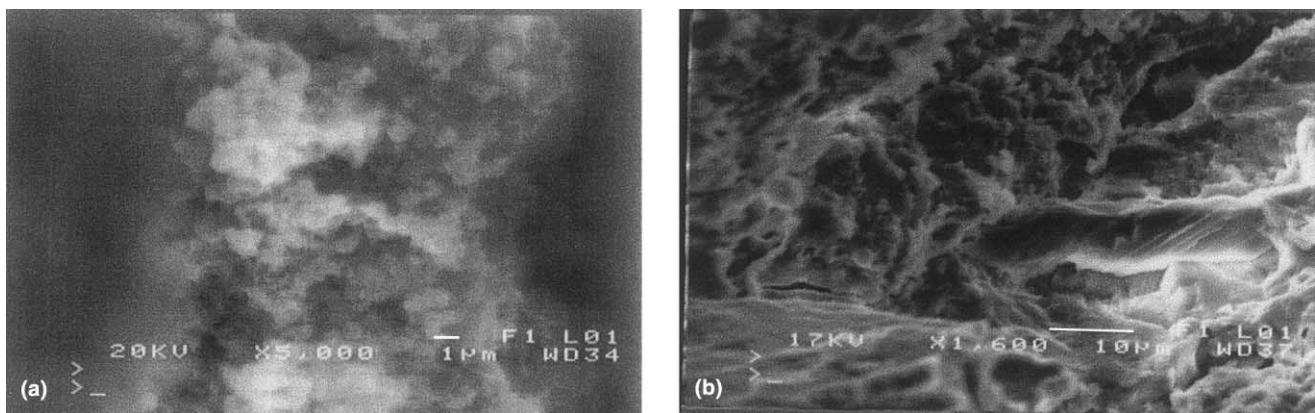


Fig. 6. (a) SEM of interface between cement mortar and SF-Ca(OH)<sub>2</sub> repair material after 2 months of hydration (M × 5000) (b) SEM of interface between cement mortar and SF-Ca(OH)<sub>2</sub> repair material after 18 months of hydration (M × 1600).

showed free corrosion potentials in the range of -330 to -370 mV. Thereafter a decay to more negative potential values was observed which lasted from 4 to 7 days depending on the type of the specimens. Afterwards a

more or less steady-state situation is observed and the potential values remain almost stable around -750 mV. The potential decay to high negative values could be attributed to the experimental conditions, i.e. to the

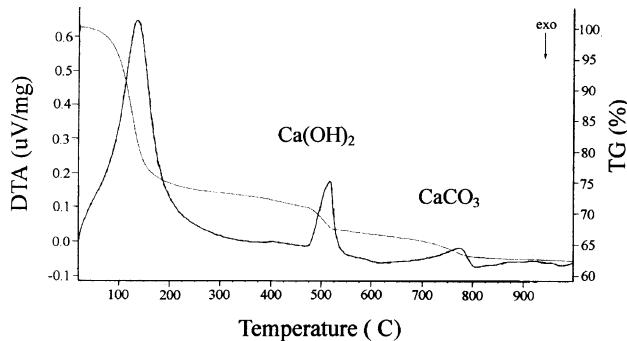


Fig. 7. DTA-TG diagram of a 3 months hydrated of SF- $\text{Ca}(\text{OH})_2$  repair mixture.

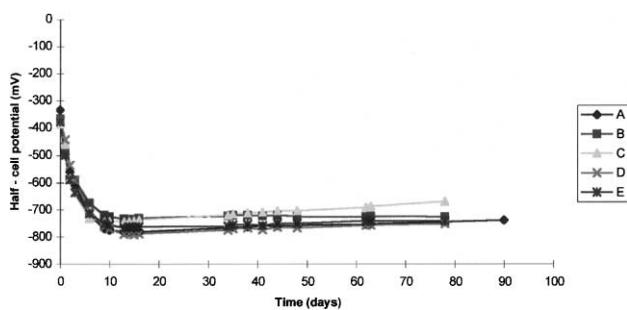


Fig. 8. Half cell potential versus immersion time.

total immersion of the specimens into the  $\text{NaCl}$  solution, which leads to limited availability of oxygen and thus to cathodic polarization increase [20–22].

Regarding the significance of the numerical value of the potentials, it is well established (ASTM C876), that if corrosion potentials are numerically greater than  $-275$  mV versus SCE, there is a greater than 90% probability that corrosion of reinforcing steel bars occurs. Thus from Fig. 8, it is clear that this condition appears in all types of specimens. The small differences in plateau values do not permit any clear qualitative prediction of differences in the behavior of the different types of specimens.

Among the laboratory tests, that of the mass loss measurement versus the exposure time provides the ability of a rather correct prediction of a construction lifetime. The results of these measurements for all types of specimens tested are presented in Fig. 9.

The situation displayed in Fig. 9 reveals that the mass loss of the rebars increases with exposure time in all types of specimens. The increase of the undamaged specimens is rather regular. In contrast to this, the damaged but not repaired specimens exhibit increased mass loss values by a factor of about 3, from the beginning of the exposure.

In all types of repaired specimens, throughout the whole exposure time, the corrosion rate is relatively higher than that of undamaged ones, due to the porosity

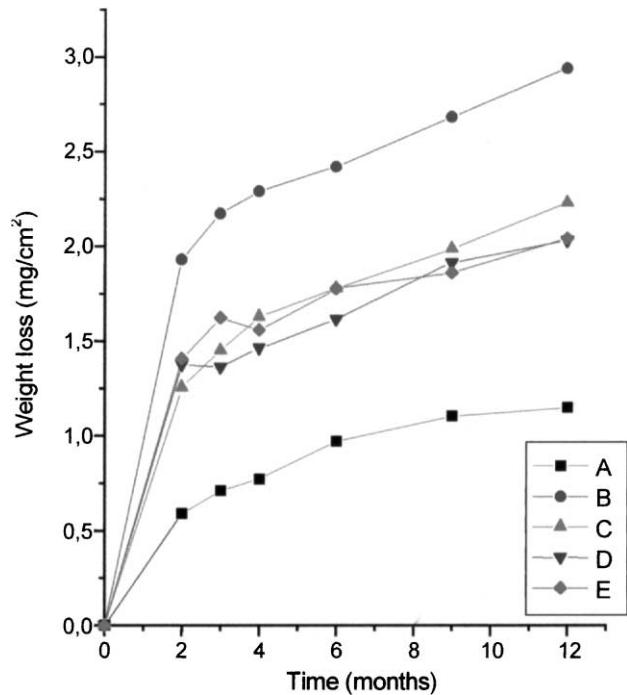


Fig. 9. Weight loss of steel rebars versus exposure time.

of the repair mixtures in the early age of their hydration [23]. Nevertheless it remains always lower than the corresponding one to damaged but not repaired specimens. The above results lead to the conclusion that the use of these repair mixtures improves the concrete behavior and consequently the corrosion performance of the steel rebars. The differences in the corrosion rate values of the repaired specimens are very low indicating similar behavior of all types of repair – mixtures. Both the damaged but not repaired specimens and the repaired ones exhibit very intense mass loss increase during the first two months of exposure. This may be due to the fact that, during this early stage period, the formation of C-S-H products is low. After this period, the hydration reactions have proceeded to an appropriate extent which evidently creates products at the interface between mortar-repair mixture possessing good binding properties.

The influence of the presence of the hydration products at the interface mortar-repair mixture on the corrosion performance of the steel rebars is also estimated by electrochemical measurement of their corrosion rate.

The corrosion current density of steel rebars against time of immersion is given in Fig. 10. These results are in line with the above-mentioned ones of the weight loss measurements. The corrosion rate of the damaged but not repaired specimens, (B), is about two times higher than the corrosion rate of undamaged specimens (A). The corrosion rates in the repaired specimens are relatively higher than those in the undamaged ones but, in

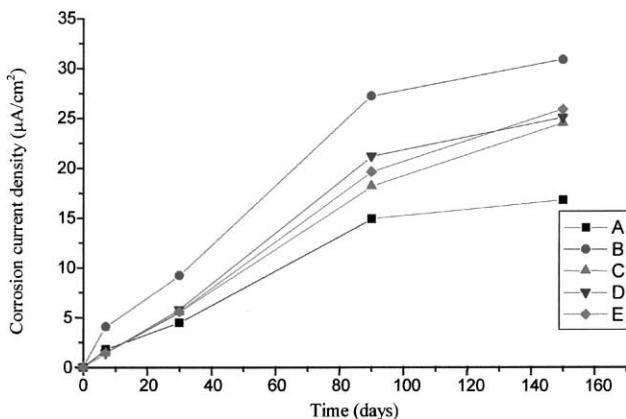


Fig. 10. Corrosion current density versus immersion time.

any case, lower than those in damaged but not repaired specimens. As this condition is valid for all types of repaired specimens it could be concluded that all three types of repair mixtures possess almost same properties leading to similar behavior.

The carbonation depth of all types of specimens was measured at the interface of the mortar-repair mixture in order to estimate the quality of products created in this interface which can influence the deterioration process of concrete structure (Fig. 11). As it is shown in Fig. 11 the undamaged mortar specimens present very low carbonation depth, which does not change significantly after the three first months of exposure in atmosphere. In damaged but not repaired specimens, after a

short time of exposure, about one month, the carbonation depth has reached the maximum depth of the hole and thereafter continues going deeper into the steel mortar cover. Nevertheless at the end of the exposure the carbonation has not reached the steel rebars. On the contrary, in repaired specimens, the carbonation depth changes a little with exposure time remaining always close to that of the undamaged specimens. This could be attributed to the rehabilitation of the structure of the damaged specimens to an extent close to that of the undamaged one. This rehabilitation is the result of the formation of calcium silicate hydrates of some importance both in the case of pure SF-Ca(OH)<sub>2</sub> repair mixtures, as well as in mixtures containing cement as it is proved by XRD and SEM measurements. Additionally, these measurements have shown that these hydrates are well crystallized on the surface of the hole and that they exhibit good binding properties.

The comparison of Figs. 9 and 11 indicates that the behavior of the repaired specimens is influenced more by the ingress of chloride ions than by the atmospheric carbon dioxide access. This suggests that special care should be given to the protection of steel rebars from corrosion depending on the corrosion environment i.e. on the place where the construction is located.

#### 4. Conclusions

The present approach to the problem of the choice of alternative mixtures as concrete repair materials instead of usual cementitious ones leads to the following conclusions:

1. During the hydration of SF-Ca(OH)<sub>2</sub> mixtures calcium silicate hydrates are formed in an appropriate extent, creating good binding properties to the repair mixtures.
2. The addition of some amount of cement to these mixtures provides better setting time.
3. Repaired specimens exhibit low carbonation depth in all cases.
4. In a corrosive environment of NaCl solution, corrosion rate of steel rebars of the repaired specimens with pure SF-Ca(OH)<sub>2</sub> mixture, as well as with mixtures containing cement, is higher than that of undamaged specimens but remains always about half of that of damaged but not repaired specimens.

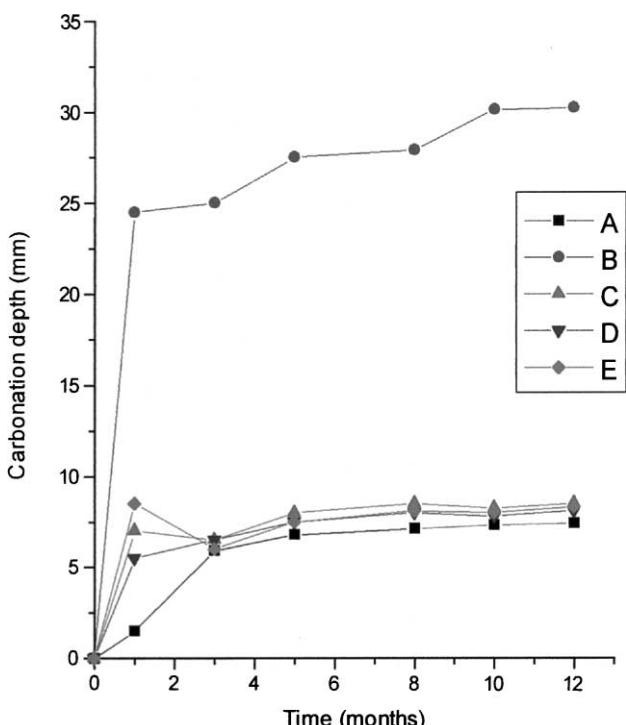


Fig. 11. Carbonation depth time dependence.

#### References

- [1] Lea FM. The chemistry of cement and concrete. 3rd ed. Great Britain: Edward Arnold; 1970. p. 553.
- [2] Gonzalez JA, Molina A, Otero E, Lopez W. On the mechanism of steel corrosion in concrete: the role of oxygen diffusion. Mag Concr Res 1990;42(159):23–7.

- [3] Wenger F, Galland I. EIS study of the protective properties of repair products. In: Proceedings of the Eurocorr'96;Session I: Corrosion in concrete. Nice: 1996; P. I OR 8-1.
- [4] Byfors K. Influence of silica fume and fly ash on chloride diffusion and pH values in cement paste. *Cem Concr Res* 1987;17:115–30.
- [5] Wheat HG, Eliezer Z. Some electrochemical aspects on corrosion of steel in concrete. *Corrosion-NACE* 1985;41(11):640–5.
- [6] Kouloumbi N, Batis G. Chloride corrosion of steel rebars in mortars with fly ash admixtures. *Cem Concr Compos* 1993;14:199–207.
- [7] Miyagawa T. Durability design and repair of concrete structure: chloride corrosion of reinforcing steel and alkali-aggregate reaction. *Mag Concr Res* 1991;43(156):155–70.
- [8] Sorensen B, Maahn E. Penetration rate of chloride in marine concrete structures. Publication 1, *Nordic Concr Res* 1982;24.1–24.18.
- [9] Malami CH, Batis G, Kouloumbi N, Kaloidas V. Influence of pozzolanic and hydraulic cement additions on carbonation and corrosion of reinforced mortar specimens. In: Swamy RN, editor. *Proceedings of the International Conference Corrosion Protection of Steel in Concrete*. Sheffield; 1994. II p. 668–82.
- [10] Kouloumbi N, Batis G, Malami CH. The anticorrosive effect of fly ash, slag and a greek pozzolan in reinforced concrete. *Cem Concr Compos* 1994;16:253–60.
- [11] Malami CH, Kaloidas V, Batis G, Kouloumbi N. Carbonation and porosity of mortar specimens with pozzolanic and hydraulic cement admixtures. *Cem Concr Res* 1994;24(8):1444–54.
- [12] Gudmundsson G, Olafsson H. Silica Fume in concrete-16 years of experience in iceland, alkali-aggregate reaction in concrete. In: Shayan A, editor. *Proceedings of the 10th International Conference*. Melbourne; 1996. p. 462–69.
- [13] Lagerblad B, Utkin P. Silica granulates in concrete-dispersion and durability aspects. CBI Report 3.93. Swedish Cement and Concrete Research Institute, 1993, p. 44.
- [14] Marusin SL, Shotwell LB. Alkali-Silica reaction in concrete caused by densified silica fume lumps-a case study In: *Proceedings of the Fifth CANMET/ACI International Conference on Fly Ash, Silica Fume, Slag and Natural Pozzolans in Concrete. Supplementary Volume*, Milwaukee; 1995. p. 45–59.
- [15] Takemoto K, Uchikawa H., Hydration of pozzolanic cement. In: *Seventh International Congress on the Chemistry of Cement*. Paris; 1980. Vol. I., IV-2.
- [16] Kasselouri V, Parissakis G. Stabilization of magnesia cements by adding flying ashes and slag. *Silicate Indust* 1977;1:13–7.
- [17] NaraiSabo, I. *Inorganic crystallochemistry*, Ac. Sc. Publ Budapest; 1969.
- [18] Ftikos CH, Kasselouri V, Tsimas C, Parissakis G. A study on the action of seawater on hydrated cement pastes. In: *Proceedings of the Seventh Congres, International de la Chimie des Ciments*, Vol. IV; 1980.
- [19] Kasselouri V, Ftikos CH, Parissakis G. DTA-TG Study on the  $\text{Ca}(\text{OH})_2$ -Pozzolan reaction on cement pastes hydrated up to three years. *Cem Concr Res* 1983;13:649–54.
- [20] Montemor MF, Simoes AMP, Salta MM, Ferreira MGS. Electrochemical behavior of fly ash containing concrete by impedance spectroscopy. In: Costa JM, Mercer AD, editors. *Progress in the Understanding and Preventing of Corrosion*. 10th European Corrosion Congress, vol. 1. Barcelona: The Institute of Materials; 1993. p. 642–51.
- [21] Maslehuddin M, Al-Mana AI, Saricimen H, Shamim M. Corrosion of reinforcing steel in concrete containing slag or pozzolans. *Cem Concr Aggreg CCAGDP* 1990;12(1):24–31.
- [22] Batis G, Kouloumbi N, Malami CH. Corrosion resistance of steel rebars in mortar specimens with santorin earth, OEBALIA, Vol XIX; 1993. p. 53–60.
- [23] Kasselouri-Rigopoulou V, Kouloumbi N, Papadakis V, Sioutis S. Permeability study of various aggressive media in repaired concretes. In: Yeginobali A, editor. *Cement and Concrete Technology in the 2000s*. II International Symposium, Vol. 2. Istanbul; 2000. p. 332–40.